Dependence of reaction rate of pyrite oxidation on temperature, pH and oxidant concentration

LU Long[1], WANG Rucheng[2], XUE Jiyue[2], CHEN Fanrong[1] & CHEN Jun[2]

1. Guangzhou Institute of Geochemistry, Chinese Academy of Sciences, Guangzhou 510640, China;
2. Department of Earth Sciences, Nanjing University, Nanjing 210093, China
Correspondence should be addressed to Lu Long (email: lulong@gig.ac.cn)

Received Jannuary 17, 2004; revised December 28, 2004

Abstract The kinetic sstudy of pyrite oxidation was performed in a series of experiments by a mixed flow reactor. The release rates of Fe(II) are in the order of $3.22\times10^{-9}-5.51\times10^{-7}$ $mol\cdot m^{-2}\cdot s^{-1}$ at temperature (T) 25 to 44℃, initial pH (pH)1.4 to 2.7, and initial Fe(III) concentration ($[Fe(III)]_i$) 10^{-5} to 5×10^{-3} $mol\cdot kg^{-1}$. The release rate of Fe(II) increased with increasing T or/and pH or/and $[Fe(III)]_i$ in the above range. The rate law and activation energy of pyrite oxidation were derived by statistical analyses of $R_{Fe(II)}$ vs. $[Fe(III)]_i$, RFe(II) vs. pH and $R_{Fe(II)}$ vs. T, and are given as (1) Rate law: $R_{Fe(II)}=10^{4.65}e^{-64.54\times10^3/8.31T}\frac{[Fe(III)]_i^{0.60}}{[H^+]^{0.45}}$; (2) activation energy: 64.54 ± 8.07 $kJ\cdot mol^{-1}$. The expression can be applied to more cases (e.g., quantifying the pollutant released from sulfide-rich mining waste and assessing reliable performance of underground repository sites where pyrite acts as an engineered barrier material). Using the rate law derived from this study, the magnitude of the pollutants transferred to secondary phases, soil and water from oxidized pyrite during Jiguanshan mine waste weathering was preliminarily estimated. The estimated magnitude is very high, suggesting that the pile has possibly posed significant impact on the water quality in this region.

Keywords: temperature, oxidant concentration, pH, oxidation rate, pyrite, environmental effect.

DOI: 10.1360/02yd0115

Pyrite is a common sulfide mineral, particularly abundant in mining waste. It is a focus of mine environmental concern because the oxidation of exposed pyrite may lead to acid drainage and poisonous materials (like As and heavy metals) release. In the United States, approximately $1000000 per day is spent in alleviating acid mine drainage[1], while the Canadian mining community has environmental liabilities that exceed $2 billion for disposal, management, and reclamation of mine waste[2]. Pyrite has been considered to be the main contributor of acid and heavy metal from mining wastes[3]. Thus, a better knowledge on the oxidation kinetics of pyrite is very important in predicting long-term environmental loading of acid and heavy metals from mining waste, assessing the potential effectiveness of various waste-rock management alternatives, and providing insights into oxidation mechanism.

Pyrite, presented in the wall rock of repository sites and in bentonite surrounding the waste containers, acts

as an engineered barrier material of the disposal system because it consumes oxidant (e.g., DO and ferric iron) in groundwater and prevents radionuclides from release[1]. Thus, a rate law of pyrite oxidation is necessary for reliable performance assessment of underground repository sites.

An underground repository, influenced by heat from fission reaction of nuclear waste and by geothermal gradient, is of higher temperature than room temperature (usually up to 70℃)[2]. Relative to pH and oxidant concentration, temperature contributes more impact to the oxidation rate of pyrite in the disposal system. Most of previous studies were conducted at room temperature[4−10][3], and also none of them investigated rate dependence on temperature. Consequently, rate expression of pyrite oxidation derived by these researchers cannot be applied to calculating the oxidation rates of pyrite in the disposal system of nuclear waste and quantifying pollutant release from tailings.

We systemically performed a kinetic study of pyrite oxidation by a mixed flow reactor based on understanding mentioned above. We report here the results of our experiments, and derive rate expression of pyrite oxidation by ferric iron, which expresses the dependence of oxidation rate of pyrite on temperature. The expression can be applied to more cases.

1 Materials and methods

1.1 Samples

Pyrites used in this study were obtained from Jiguanshan waste rock dump in Tongling, Anhui, China. The pyrites ranging from 1 to 2 mm size were sorted for experiments. The chosen samples were immersed 8 h in 1 N hydrochloric acid to dissolve any carbonate and oxide coating, washed by ultrasonic in deionized water, and dried in air. Next, the samples crushed by gently grinding in an agate mortar using an agate pestle. A size fraction of 150−250 μm was selected through sieving. Pretreatment for this size fraction sample is similar to those reported by McKibben (1986), Rimstidt (1993) and Janzen (2000)[7,8,11]. The selected powder samples were washed by deionized water and cleaned in ethanol by ultrasonic to remove fine grains adhered to crystals. Next, the samples were soaked in hydrochloric acid to remove oxidation coating. Then the samples were rinsed with deionized water followed by acetone, dried and stored.

Bulk composition of pyrite determined by electron microprobe analysis using a Jeol JXA-8800 superprobe (wt%, mean value of 26 analysis points), was: S, 52.73; Fe, 46.3; As, 0.08; Cu, 0.03; Pb, 0.05; Co, 0.08; Bi, 0.17; Zn, Ni and other metals, under detection limits[12].

Ferric sulfate solutions were prepared by oxidizing ferrous sulfate with H_2O_2, and contain essentially no Fe(II) (confirmed by our analysis). Fe(III) solution was diluted to desired concentration with di-deionized water. The pH of solution was adjusted by sulfuric acid to desired value. All of reagents used above are of analytical reagent-grade. Feed solution was purged with Ar for about 2 h to remove DO prior to experiment.

1.2 Experimental device

Mixed flow reactor experiments can directly measure reaction rates, thus their results can be fit to the differential rate law without further processing, while batch reactor and plug flow reactor experimental data must be differentiated to determine reaction rates before rates are fit to the differential rate law[8]. Apparently, a mixed flow reactor is preferable for the study of mineral reaction kinetics due to its simplicity during experiment and data analysis[13,14].

1) Power Reactor and Nuclear Fuel Development Corporation, Reseach and development on geological disposal of high-level radioactive waste, First Progress Report, 1992, PNC TN 1410, 93-053.

2) Smith, E. E., Shumate, K. S., Report by the Otio State Research Foundation for the Federal Water Pollution Control Administration, Program No. FWPCA, Grant No. 14010, FPS, 1970.

3) Luo Xingzhang, Geochemistry of the pre-selected Beishan area for high-level radioactive waste repository of China, Doctoral Thesis of Nanjing University, 2002.

The reactor used in the experiments is a mixed flow reactor designed by Institute of Geochemistry, Chinese Academy of Sciences. It is a device accompanying with side arm, stirred continuously by a rising airflow. Yu et al. (2003) described the device in detail[15]. Experiments were conducted under Ar atmosphere. The flux of Ar purged was 0.5 $L \cdot min^{-1}$, and the flow rate of solution ranged 5.0—6.0 $mL \cdot min^{-1}$, yielding a residence time (θ) with the cell of about 2.0—2.5 h. Purging Ar during the reaction played flowing roles: (1) The reaction was held under no oxygen; and (2) the reaction solution was stirred, and pyrite was maintained in suspension to improve the contact between pyrite and solution and to reduce the crack resulting from collision and attrition.

1.3 Experimental and analytical method

The study was conducted to determine the effect of Fe(III) concentration, pH and temperature on the oxidation rate of pyrite, and disregarded the effect of the concentration of DO and Fe(II). In fact, the investigation of McKibben (1986) indicated that ferrous iron concentration influenced negligibly the oxidation rate of pyrite[7]. The data of Moses (1991) showed that the contribution of DO to the oxidation rate of pyrite was 1/15 of the contribution of ferric iron[16].

The solution of desired pH and Fe(III) concentration was added into reactor till to the height of 750 mL level. The reactor was sealed and immersed in constant-temperature (25℃, 36℃ or 44℃; ±0.5℃) water bath. Ar was charged, and one gram of pyrite was added, to the reactor, after Eh reached a steady state. Then, the experiment began, and Eh and time were recorded. The previous experiments using this device showed that the reaction could arrive at the steady state as it lasted one residence time (1θ)[13]. The study of Lengke (2001) indicated that pH, Eh, the release amount of S and As did not reach a steady state at the same time, but all of them had reached the steady state after the reaction lasted 4.5 h (approximately 4.5θ)[17]. The time span of experiments in this study was 15—20 h (approximately $7-8\theta$). The reaction rates were determined from composition analyses of the effluent solution close to the end of the experiment.

The pH of solution was checked before and after each experiment. The pH values of feed solution in this study were kept intentionally lower than 2.7 to prevent from hydrolyzation of ferric iron and precipitation of ferric hydroxide.

Concentrations of ferrous iron and total iron were determined spectrophotometrically in a 1,10-phenanthroline medium[18]. Surface area measurements of pyrite were performed in a Micromeritics ASAP 2010 M+C BET surface area analyzer by N_2 adsorption. The specific surface area of pyrite samples is 0.05 ± 0.005 m^2/g.

1.4 Calculation of reaction rates and statistical analyses of data

The previous studies show the stoichiometric reaction for pyrite oxidation by Fe^{3+} is

$$FeS_2 + 14Fe^{3+} \Rightarrow 15Fe^{2+} + 2SO_4^{2-} + 16H^+ \quad (1)$$

Steady state oxidation rates in a mixed flow reactor were calculated using the following equation[8,13,14,19]:

$$R_j = (C_{jo} - C_{ji})\, r_f / A, \quad (2)$$

where R_j is the reaction rate of component j in solution ($mole \cdot m^{-2} \cdot s^{-1}$). C_{jo}, C_{ji} are the output concentration of steady state and the input concentration of component j ($mol \cdot kg^{-1}$), respectively, r_f is the flow rate of the solution through the system ($kg \cdot s^{-1}$), and A is the total surface area of solid sample (m^2).

As usual[7—11,15], the double-logarithmic plot was used as a method of data analysis to derive a general rate law in this study.

2 Results and discussion

2.1 Reaction progress variable

Reaction progress variable was usually chosen from three variables—the release amount of $[SO_4]^{2-}$, of Fe(II), and the consumed amount of Fe(III) in the rate calculation of pyrite oxidation. S in sulfide minerals is usually oxidized into elemental sulfur, sulfate and other intermediate sulfoxy anions, and the calculated

rates based on the release of sulfate are less than true rates[11,17]. Thereby, the release amount of $[SO_4]^{2-}$ is not taken as RPV in this study. Moses et al. (1991) used the consumed amount of Fe(III) as RPV under the condition of circumneutral pH. They concluded that the increasing content of Fe^{2+} in solution is less than the Fe^{2+} amount released from reaction, and thus, the rate calculated upon the amount of released Fe^{2+} is less than the true rate of the reaction, assuming that Fe^{2+} is preferentially adsorbed on the surface of pyrite relative to Fe^{3+} [16]. In the study, the rates calculated upon the release amount of Fe(II) and those upon the consumed amount of Fe(III) from the identical experiment were compared in a few experiments, and there is little difference, suggesting that the adsorbed Fe^{2+} should be little. An explanation is that medium of acidic pH in this study does not favor the adsorption of Fe^{2+} to pyrite surface. The study of McKibben (1986) indicated that Fe^{2+} is not oxidized to Fe^{3+} in the air during 4 days[7]. Accordingly, that release amount of Fe(II) or the consumed amount of Fe(III) was used as RPV should result in little difference. In fact, using the release amount of Fe(II)[7,11] or the consumed amount of Fe(III)[8,9] as RPV had acquired comparable results in the kinetic studies of pyrite oxidation conducted in acidic medium. However, it is noted that the consumed Fe(III) is usually the tenth of initial Fe(III) concentration, even down to 5% in a few of our experiments. The magnitude is close to the level of analytical error. But the amount and variation of released Fe(II) in different experiments can be distinctly determined with feed of no Fe(II). Consequently, the release amount of Fe(II) is chosen as PRV in our study.

2.2 Effect of $[Fe(III)]_i$ and pH

Experiments were conducted in initial Fe(III) concentrations ($[Fe(III)]_i$) range of $10^{-5} - 5 \times 10^{-3}$ $mol \cdot kg^{-1}$ with pH (=2) and temperature keeping constant to investigate effect of $[Fe(III)]_i$ on rate. The results at three various temperatures (25℃, 36℃, 44℃) are presented in Table 1. It is shown that the reaction rate increases with increasing $[Fe(III)]_i$, which suggests that pyrite surface has not reached saturation with increasing $[Fe(III)]_i$ levels in the range of $[Fe(III)]_i$ used in this study. The plots of log oxidation rate vs. log $[Fe(III)]_i$ at three different temperatures are shown in Fig. 1(a), (b), (c), respectively. The slopes and intercepts from linear regression of the data are listed in Table 2. The mean slope of linear regression at the three temperatures is 0.60 ± 0.04, which indicates a reaction order of 0.60 for $[Fe(III)]_i$.

The experiments determining the effect of pH were

Table 1 Oxidation rates of pyrite

No.	$[Fe(III)]_i$	pH	T/℃	$R_{Fe(II)}$	No.	$[Fe(III)]_i$	pH	T/℃	$R_{Fe(II)}$
MF1	9.50×10^{-4}	2.0	36	1.90×10^{-7}	MF17	5.10×10^{-3}	1.4	44	2.13×10^{-7}
MF2	9.50×10^{-4}	2.0	44	2.94×10^{-7}	MF18	4.05×10^{-3}	2.14	36	2.70×10^{-7}
MF3	9.47×10^{-5}	2.0	36	4.98×10^{-8}	MF19	3.75×10^{-3}	2.2	44	4.06×10^{-7}
MF4	2.04×10^{-4}	2.0	36	1.16×10^{-7}	MF20	1.19×10^{-4}	2.67	36	5.52×10^{-8}
MF5	1.10×10^{-4}	2.0	44	8.32×10^{-8}	MF21	1.10×10^{-4}	2.66	25	1.13×10^{-8}
MF6	1.08×10^{-5}	2.0	36	8.22×10^{-9}	MF22	1.02×10^{-4}	2.74	44	7.46×10^{-8}
MF7	6.75×10^{-5}	2.0	25	7.83×10^{-9}	MF23	9.30×10^{-5}	1.42	36	1.20×10^{-8}
MF8	9.90×10^{-4}	2.0	36	1.92×10^{-7}	MF24	1.04×10^{-4}	1.43	44	2.23×10^{-8}
MF9	9.52×10^{-4}	2.0	25	7.34×10^{-8}	MF25	1.06×10^{-5}	2.51	25	4.02×10^{-8}
MF10	2.04×10^{-3}	2.0	25	3.22×10^{-8}	MF26	1.03×10^{-5}	1.49	36	5.58×10^{-8}
MF11	1.04×10^{-3}	2.0	44	3.88×10^{-7}	MF27	9.97×10^{-4}	2.63	36	1.73×10^{-7}
MF12	1.23×10^{-4}	2.0	25	1.98×10^{-8}	MF28	1.00×10^{-5}	1.41	36	3.31×10^{-8}
MF13	3.82×10^{-3}	2.12	44	5.51×10^{-7}	MF29	9.68×10^{-4}	2.63	44	2.49×10^{-7}
MF14	4.22×10^{-3}	2.13	36	3.81×10^{-7}	MF30	1.54×10^{-3}	1.73	44	1.36×10^{-7}
MF15	4.93×10^{-3}	2.1	36	7.61×10^{-8}	MF31	4.22×10^{-3}	1.76	25	2.23×10^{-8}
MF16	5.05×10^{-3}	1.39	36	1.15×10^{-7}					

Table 2 Reaction order and rate constant of oxidation reaction of pyrite

	Logarithmic plot of rate—[Fe(III)]$_i$		Plot of rate logarithm—pH	
T/℃	$n \pm 1\sigma$	$k \pm 1\sigma$	$N \pm 1\sigma$	$k \pm 1\sigma$
25	0.60±0.11	$10\times e^{-5.53\pm0.43}$	0.43±0.07	$10\times e^{-6.69\pm0.15}$
36	0.63±0.07	$10\times e^{-4.80\pm0.24}$	0.52±0.05	$10\times e^{-6.19\pm0.10}$
44	0.55±0.08	$10\times e^{-4.87\pm0.24}$	0.41±0.04	$10\times e^{-6.02\pm0.08}$
Mean	0.60±0.04		0.45±0.03	

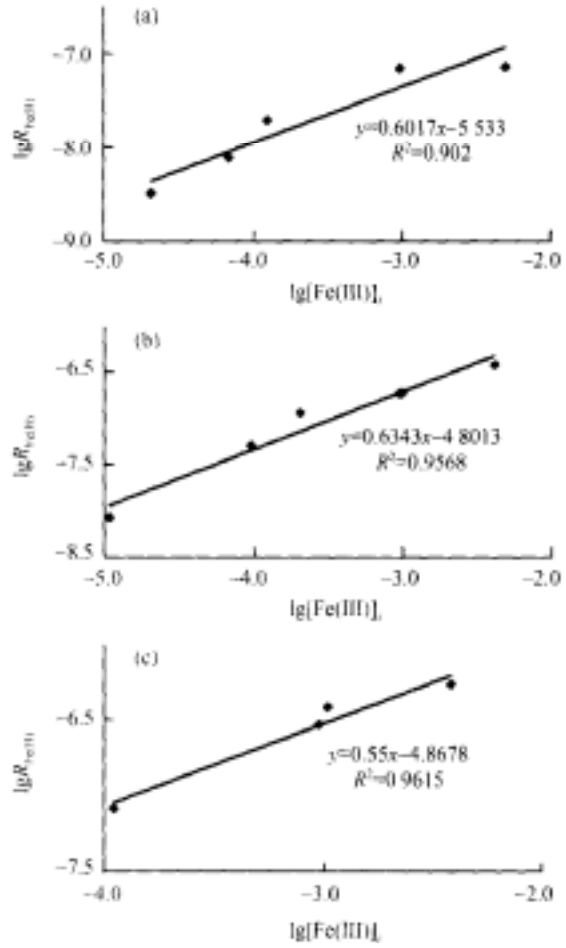

Fig. 1. Effect of [Fe(III)]$_i$ on oxidation rate of pyrite (pH=2) (25℃).

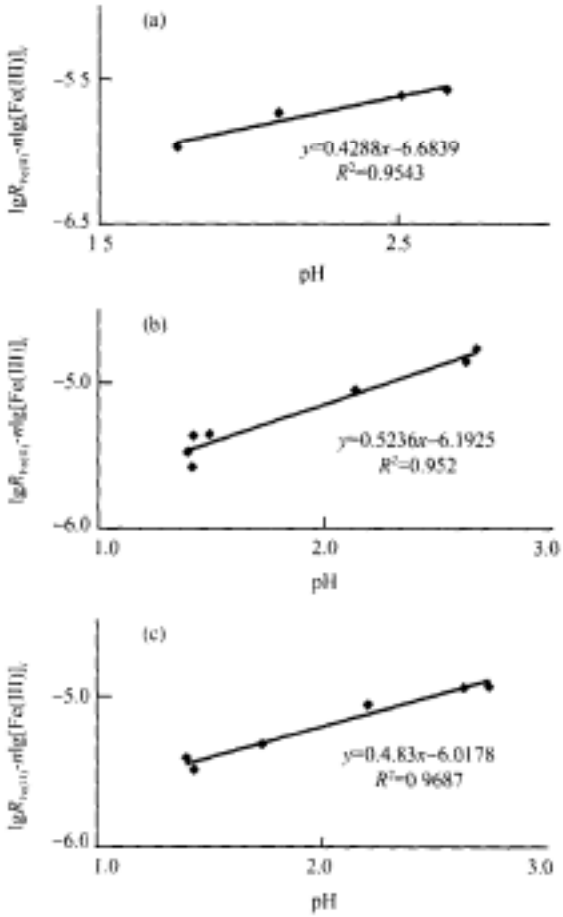

Fig. 2. Effect of pH on oxidation rate of pyrite (25℃).

performed at different initial pH (pH =1.3, 2.0, 2.7). The results are also presented in Table 1. The rate dependence on pH is illustrated in Fig. 2. Table 2 lists the results of linear regression of the data. The mean slope of linear regression under the three temperatures is 0.45±0.03, suggesting a reaction order of 0.45 for pH. Consequently, the rate law derived from this study can be expressed as

$$R_{\mathrm{Fe(II)}} = k\frac{[\mathrm{Fe(III)}]_i^{0.60\pm0.04}}{[\mathrm{H}^+]^{0.45\pm0.04}}. \quad (3)$$

2.3 Effect of temperature

The experiments of oxidation rate as a function of temperature (T=25℃, 36℃, 44℃) show that the oxidation rate of pyrite increases with increasing temperature. The rate dependence on temperature is gen-

erally expressed by the Arrhenius equation[20],

$$k = Ae^{-E_a/RT},$$

where k is the rate constant, T is temperature (K), R is gas constant ($kJ \cdot mol^{-1} \cdot K^{-1}$), A is preexponential term, and E_a is activation energy ($kJ \cdot mol^{-1}$).

The plot of the log rate constant vs. 1000/T(K) yields a slope of -3.37 ± 0.42 (Fig. 3). An activation energy of 64.54 ± 8.07 $kJ \cdot mol^{-1}$ is estimated from the slope of the line in Fig. 3. The value is similar to those of pyrrhotite ($47.7-62.5$ $kJ \cdot mol^{-1}$) oxidation by ferric iron, orpiment (59.1 $kJ \cdot mol^{-1}$) and metacinnabar (77.0 $kJ \cdot mol^{-1}$) oxidation by oxygen[11,20,21]. It is suggested that these oxidation reactions are controlled by a surface reaction mechanism with the activation energy higher than 20 $kJ \cdot mol^{-1}$. The oxidation of amorphous As_2S_3 by oxygen is a diffusion-controlled reaction since its activation energy is less than 20 $kJ \cdot mol^{-1}$[17].

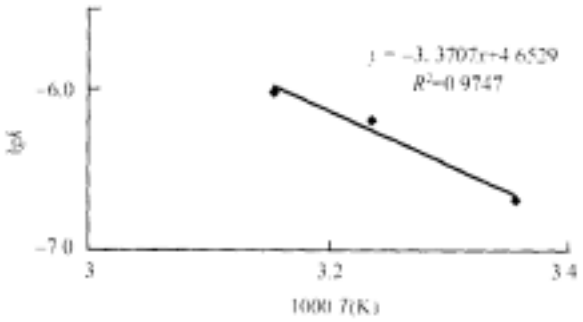

Fig. 3. Effect of temperature on the oxidation rate of pyrite.

2.4 Rate constant and rate expression

It is noticed that rate dependence on temperature was not expressed in the previous empirical rate laws. As a result, these rate laws cannot be directly applied to the conditions of other temperatures except their experimental temperatures. In the research, the rate as a function of temperature was investigated, and the relationship between rate constant and temperature is shown in Fig. 3. Activation energy of 64.54 ± 8.07 $kJ \cdot mol^{-1}$ and preexponential of 4.65 ± 1.37 in Arrhenius equation were obtained from the slope and intercept of the line in Fig. 3, respectively. Consequently, rate constant and rate expression can be described as

$$k = 10^{4.65} e^{-64.54 \times 10^3 / 8.31T},$$

and

$$R_{Fe(II)} = 10^{4.65} e^{-64.54 \times 10^3 / 8.31T} \frac{[Fe(III)]_i^{0.60}}{[H^+]^{0.45}}.$$

The rate expression can be used to calculate the oxidation rate of pyrite under various temperatures. Accordingly, it can be applied to quantifying the pollutant release from sulfide-rich mining waste and assessing reliable performance of underground repository sites where pyrite acts as an engineered barrier material.

2.5 Environmental effect of pyrite oxidation

The pollutants released from oxidized pyrites in Jiguanshan waste rock dump were calculated using the rate expression derived from this study. The calculation is described below.

It is estimated that the dump is of approximately a volume of $5 \times 10^5 m^3$, and contains pyrite of about $1.25 \times 10^8 kg$. The pyrite grains in the pile are of a mean size of 2.5 mm and a pyritohedron shape. The theoretic calculation according to the method of Parks (1990) yields the specific surface area of 4.8×10^{-4} $m^2 \cdot g^{-1}$ for these grains[22]. McGregor (1998) showed that oxygen had diffused to the depth of 1 m, and iron (Fe^{3+} and Fe^{2+}) had diffused to the depth of 10 m in Copper Cliff tailing[23]. We preliminarily estimated that the diffusing depth of ferric iron in Jiguanshan waste rock pile is 5 m using the knowledge of the moister and hotter weather, a higher porosity for waste rock relative to tailing, and less diffusing depth of ferric iron than ferrous iron. The amount of pyrites presented above the depth, which has been oxidized by ferric iron, is about 1.25×10^7 kg. The average temperature of 15℃ in a year in the region and the general ferric iron concentration of 10^{-3} $mol \cdot kg^{-1}$ and acidity of pH=3 from mine drainage were used as the parameters of calculating oxidation rate of the pyrites.

Table 3 The magnitude of pollutant released to secondary phases, soil and water from the consumed pyrites in Jiguanshan mine waste dump

	Cu	Pb	As	Co	Bi	H^+
Content in pyrite (%)	0.03	0.05	0.08	0.08	0.17	
Release amount	1.41×10^6 g	2.35×10^6 g	3.76×10^6 g	3.76×10^6 g	7.99×10^8 g	6.27×10^6 mol

The oxidation rate of the pyrite calculated (R_{py}) is 1.78×10^{-9} mol·m^{-2}·s^{-1} on the basis of the above data. Then, the magnitude of pyrite consumed by oxidation in every year can be calculated, i.e., $M = R_{py}\times$surface area$\times$time $= 1.78\times10^{-9}\times4.8\times10^{-4}\times1.25\times10^{10}\times119.96\times365\times24\times3600 = 4.04\times10^7$ g. The amount of pollutant released from the consumed pyrites is listed in Table 3.

Table 3 shows that the amount of these pollutants migrated to secondary products and/or soil and/or water from consumed pyrite is surprising. The mobility of heavy metals is controlled by many factors as solubility of heavy metals and flow rate of underground water. Thus, these calculated amounts of pollutants are only upper limit values which are possibly released to the environment. Considering vast H^+ released from oxidized pyrites, the mobility of these released heavy metals should be strong, and the fraction released to soil and/or water should be high. Consequently, the oxidation of pyrite in this pile has possibly posed significant impact on the water quality in this region.

The parameters used in the above calculation are the empirical values from previous studies or the values estimated in this study, which may have produced a significant error. The parameters of pH, ferric iron concentration, temperature, diffusing depth of ferric iron and so on need to be calibrated by measurement in field, and the data as solubility of heavy metals and flow rate of underground water should be taken into account, in future accurate calculation.

3 Conclusions

With mixed flow reactor designed by Institute of Geochemistry, Chinese Academy of Sciences, a series of experiments were conducted in the range of temperature, pH and ferric iron concentration set by this study to investigate the kinetics of pyrite oxidation. The rates obtained from these experiments are in the range of $3.22\times10^{-9}-5.51\times10^{-7}$ mol·m^{-2}·s^{-1}.

Statistically analyzing these rates by the method of double-logarithmic plot, we derived the rate law of pyrite oxidation which indicates rate dependence on temperature, and calculated activation energy of pyrite oxidation (64.54 kJ·mol^{-1}). The value of activation energy suggests that the oxidation of pyrite is controlled by surface reaction

The law can be applied to quantifying the pollutant release from sulfide-rich mining waste and assessing reliable performance of underground repository sites. Using this rate law derived from this study, magnitude of the pollutants released from oxidized pyrite in Jiguanshan mine waste dump was preliminarily estimated. The estimated magnitude is surprising.

Acknowledgements The authors would like to thank Prof. Zhu Yongxuan and Yu Yunmei for their help with experimental design and theoretic guidance, and for providing the permission to use their reaction device. This work was supported by the National Natural Science Foundation of China (Grant No. 40025209) and the Hundred Talents Program of the Chinese Academy of Sciences (Grant No. 2000[254]).

References

1. Evangeloe, V. P., Pyrite Oxidation and Its Control, Boca Raton: CRC Press, 1995, 293.
2. Holling, P., Hendry, M. J., Nicholson, R. V. et al., Quantification of oxygen consumption and sulphate release rates for waste rock piles using kinetic cells: Cluff lake uranium mine, northern Saskatchewan, Canada, Appl. Geochem., 2001, 16: 1215－1230.
3. Nesbitt, H., W., Muir, I. J., X-ray photoelectron spectroscopic studies of a pristine pyrite surface reacted with water vapour and air, Geochim. Coschim. Acta, 1994, 58: 4667－4679.
4. Garrels, R. M., Thompon, M. E., Oxidation of pyrite by iron sulfate solution, Amer. J. Sci., 1960, 258-A: 57－67.
5. Mathews, C. T., Robins, R. G., The oxidation of ferrous sulfide by ferric sulfate, Australian Chem. Eng., 1972, 13: 21－25.
6. Lowson, R. T., Aqueous oxidation of pyrite by molecular oxygen, Chem. Rev., 1982, 82: 461－497.
7. McKibben, M. A., Barnes, H. L., Oxidation of pyrite in temperature acidic solution: Rate laws and surface textures, Geochim. Coschim. Acta, 1986, 50: 1509－1520.
8. Rimstidt. J. D., Newcomb, W. D., Measurement and analysis of rate data: The rate of reaction of ferric iron with pyrite, Geochim. Coschim. Acta, 1993, 57: 1919－1934.

9. Williamson, M. A., Rimstdt, J. D., The kinetics and electrochemical rate-determining step of aqueous pyrite oxidation, Geochim. Coschim. Acta, 1994, 58: 471－482.
10. Holmes, P. R., Crundwell, F. K., The kinetics of the oxidation of pyrite by ferric ions and dissolved oxygen: An electrochemical study, Geochim. Coschim. Acta, 2000, 64: 263－274.
11. Janzen, M. P., Nicholson, R. V., Scharer, J. M., Pyrrhotite reaction kinetics: Reaction rates for oxidation by oxygen, ferric iron, and for nonoxidative dissolution, Geochim. Coschim. Acta, 2000, 64 : 1511－1522.
12. Lu, L., Wang, R. C., Xue, J. Y., Chen, J., Activity of elements during the weathering of pyrite and its environmental effects, Geological Review (in Chinese with English abstract), 2001, 47: 95－101.
13. Yu, Y. M., Zhu, Y. X., Gao, Z. M., A kinetic study of oxidation of arsenopyrite in acidic solutions: 1. experimental method and some results, Acta Mineralogica Sinca (in Chinese with English abstract), 2000, 20(4): 90－395.
14. Zhang, S., Li, T. J., Wang, L. K., The theory of geochemical kinetic reactor and determination of rate equation: An introduction., Geology-Geochemistry (in Chinese with English abstract), 1997, (1): 53－59.
15. Yu, Y. M., Zhu, Y. X., Williams, J. A. E., et al. A kinetics study of the oxidation of arsenopyrite in acidic solutions: implications for the environment, Appl. Geochem., 2003, 19: 435－444.
16. Moses, C. O., Herman, J. S., Pyrite oxidation at circumneutral pH, Geochim. Coschim. Acta, 1991, 55: 471－482.
17. Lengke, M. F., Tempel, R. N., Kinetic rates of amorphous As_2S_3 oxidation at 25 to 45℃ and initial pH of 7.3 to 9.4, Geochim. Coschim. Acta, 2001, 65: 2241－225.
18. Marczenko, Z., Spectrophotometric Determination of Elements, New York: John Wiley and Sons, 1976.
19. Ganor, J., Mogollon, J. L., Lasaga, A. C., Kinetics of gibbsite dissolution under low ionic strength conditions, Geochim. Coschim. Acta, 1999, 63: 1635－1651.
20. Lengke, M. F., Temple, R. N., Reaction rates of natural orpiment oxidation at 25 to 40℃ and pH 6.8 to 8.2 and comparison with amorphous As_2S_3 oxidation, Geochim. Coschim. Acta, 2002, 66:3281－3291.
21. Barnett, M. O., Turner, R. R., Singer, P. C., Oxidative dissolution of metacinnabar (β-HgS) by dissolved oxygen, Appl. Geochem., 2001, 16: 1499－1512.
22. Parks, G. A., Surface energy and adsorption at mineral / water interface: An introduction, in: Mineral-water Interface Geochemistry, Reviews in Mineralogy (eds. Hochella and White), 1990, 23: 133－175.
23. McGregor, R. G., Blowes, D. W., Jambor, J. L., The Solid–phase controls on the mobility of heavy metals at the Copper Cliff tailing aera, Sudbury, Ontario, Canada, Journal of Contaminant Hydrology, 1998, 33: 247－271.